ON SOME ASPECTS OF LEVITATION HEATING OF METAL BODIES

*Martin MACH, *Pavel KARBAN, **Ivo DOLEŽEL
*Faculty of Electrical Engineering UWB, Univerzitní 26, 306 14 Plzeň, Czech Republic, E-mail: {mach, karban}@kte.zcu.cz
**Institute of Electrical Engineering AS CR, Dolejškova 5, 182 02 Prague, Czech Republic, E-mail: dolezel@iee.cas.cz

SUMMARY

Levitation induction heating represents the first step of levitation melting, which is an advanced technology used for processing of superclean metals or metal alloys. A workpiece is lifted by the Lorentz forces in time variable magnetic field produced by a system of suitably placed field coils and then heated by the Joule losses. The paper deals with optimization of the heating process from the viewpoint of the velocity of heating the workpiece. Investigated is the influence of its shape (sphere, cylinder, truncated cone) and arrangement of the field coil. The theoretical analysis is supplemented by a series of particular examples and discussion of the results obtained.

Keywords: *electrodynamic levitation, induction heating, magnetic field, temperature field, eddy currents*

1. INTRODUCTION

Heat treatment of metals or their alloys based on electromagnetic induction belongs nowadays to fast developing industrial technologies. Mentioned can be various techniques applied to solid metal bodies (hardening, drying, tempering, hot pressing) and molten metals (melting, stirring, casting, shaping, dosing). Design of the corresponding devices and production lines that must work reliably and effectively is, however, not an easy business, and still represents a challenge. The main reason is that the above processes are characterized by interaction of several physical fields that affect one another and quantitative evaluation of these phenomena is, therefore, extremely complicated.

Levitation heating mostly represents the first part of high temperature melting of strongly reactive alloys (titanium aluminides and some others) that are used in space research, chemistry, medicine etc. The main purpose of this kind of treatment is to prevent the mentioned alloys from contacting with ceramic crucible wall (as is usual in other melting techniques) and, therefore, their contamination. The process is often realized either in vacuum or suitable inert atmosphere (nitrogen, argon) contributing to high purity of the resultant material.

The technology requires a suitable system of one or more inductors producing time varying magnetic field. Eddy currents induced in the metal body inserted into this field generate in it both the Joule losses and Lorentz forces. The workpiece is first lifted into a stabilized position characterized by the balance of the Lorentz and gravitational forces, heated and finally molten.

A system containing only one inductor is not too advantageous because of rather limited possibility of controlling the process (changed can be only parameters of the field current). Moreover, lifting of the body is mostly accompanied by long-term slowly damped oscillations characterized by considerable velocities, which decelerates its heating. More efficient are, therefore, systems with more coils (their minimum number being two).

The paper represents the basic study of levitation heating of a metal workpiece in an arrangement consisting of one or two conical inductors carrying harmonic currents of the same frequency. Investigated is the influence of arrangement of the field coils on velocity of its heating. The theoretical considerations are supplemented with several illustrative examples and discussion of its results.

2. FORMULATION OF THE PROBLEM

Consider a simple axisymmetric levitating system depicted in Fig. 1. The system consists of two field coils **1, 2** and processed body **3** (considered will be a sphere, cylinder and truncated cone) that are nonmagnetic.

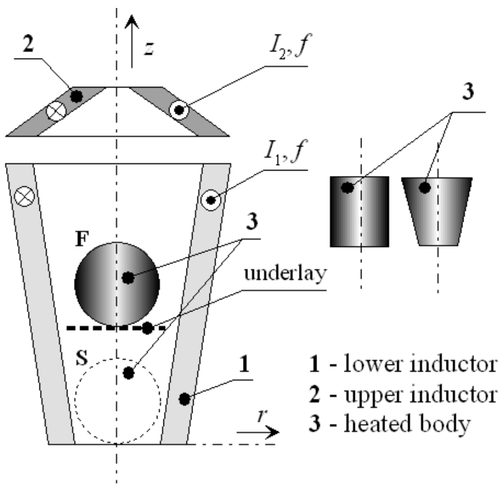

Fig. 1 The investigated arrangement

At the time $t = 0$ both coils are connected to the sources of harmonic current. The first one carries current of amplitude I_1, the second one I_2 (these amplitudes are supposed to be known and constant during the whole process), both of frequency f. These currents start producing harmonic magnetic field whose distribution also depends on mutual phase shift of both currents. This field induces eddy

ISSN 1335-8243 © 2005 Faculty of Electrical Engineering and Informatics, Technical University of Košice, Slovak Republic

currents $\boldsymbol{J}_{\mathrm{eddy}}$ in body **3**. Interaction between the magnetic field and eddy currents induced in the body produces the Lorentz forces that make it move up from the starting position **S** (marked in Fig. 1 by the dotted line) to the final position **F** characterized by the balance of the Lorentz and gravitational forces acting on it. The transient is a very complicated function of time and generally takes a period t_1. At this position the body continues to be heated up to its melting temperature T_{M}.

The temperature rise of the inductor and, particularly, processed body affects the physical properties of the system, among others electrical conductivities of its parts. Their variations influence distribution of magnetic field and, consequently, the position **F**. On the other hand, these variations are relatively small and in most cases may be neglected.

The aim of the paper representing a continuation of [1], [2] and [3] is to evaluate the whole process of heating from the viewpoint of its velocity and overall efficiency. Investigated is particularly the influence of the shape of the heated body, the shape of both coils and amplitudes of the field currents. Neglected is here the influence of the mechanical transient, in other words we assume that the starting position of the body **S** is equal to its final position **F** (it can be heated, for example, on a suitable ceramic underlay indicated in Fig. 1 by the dashed line).

3. MATHEMATICAL MODEL AND ITS SOLUTION

The mathematical model of the problem generally consists of two partial differential equations describing distribution of harmonic electromagnetic and nonstationary temperature fields in selected parts of the system.

The definition area of *electromagnetic field* is depicted in Fig. 2. Line ABCD is an artificial boundary of the arrangement that represents the infinity (position of this boundary follows from several preliminary computations showing when the field distribution near and inside the inductors no longer depends on its distance). The investigated domain contains six subregions $\Omega_{11}, \Omega_{12}, \Omega_2, \Omega_{31}, \Omega_{32}, \Omega_4$ with generally different physical parameters.

As the system is linear (in our case it contains no ferromagnetic parts), the electromagnetic field distribution is generally described by the Helmholtz equation for the phasor of vector potential $\boldsymbol{A}$ in the form [4], [5]

$$\mathrm{curlcurl}\,\underline{\boldsymbol{A}} + \mathrm{j}\cdot\mu_0\omega\gamma\underline{\boldsymbol{A}} = \mu_0\underline{\boldsymbol{J}}_{\mathrm{ext}}\,. \tag{1}$$

where γ denotes the electrical conductivity (which is a function of temperature T), $\mu_0 = 4\pi\cdot 10^{-7}$ H/m is the magnetic permeability of vacuum, ω the angular frequency of the field currents and $\underline{\boldsymbol{J}}_{\mathrm{ext}}$ their density.

The arrangement is practically axisymmetric, so that vector potential and densities of field and eddy currents have only one nonzero component in tangential direction φ_0 that may be denoted as A_φ and $J_{\mathrm{ext},\varphi}$, respectively. Now (1) can be rewritten as

$$\frac{\partial^2 \underline{A}_\varphi}{\partial r^2} + \frac{1}{r}\frac{\partial \underline{A}_\varphi}{\partial r} - \frac{\underline{A}_\varphi}{r^2} + \frac{\partial^2 \underline{A}_\varphi}{\partial z^2} + \underline{k}^2\underline{A}_\varphi = -\mu_0 \underline{J}_{\mathrm{ext},\varphi},$$
$$\underline{k}^2 = -\mathrm{j}\cdot\omega\gamma\mu_0 \tag{2}$$

The conditions along the boundary ABCDA read

- AD - antisymmetry, $\underline{A}_\varphi = 0$,
- ABCD - a force line along which $\underline{A}_\varphi = \mathrm{const}$. The condition of continuity of the vector potential at points A and D implies that this constant is identically equal to zero.

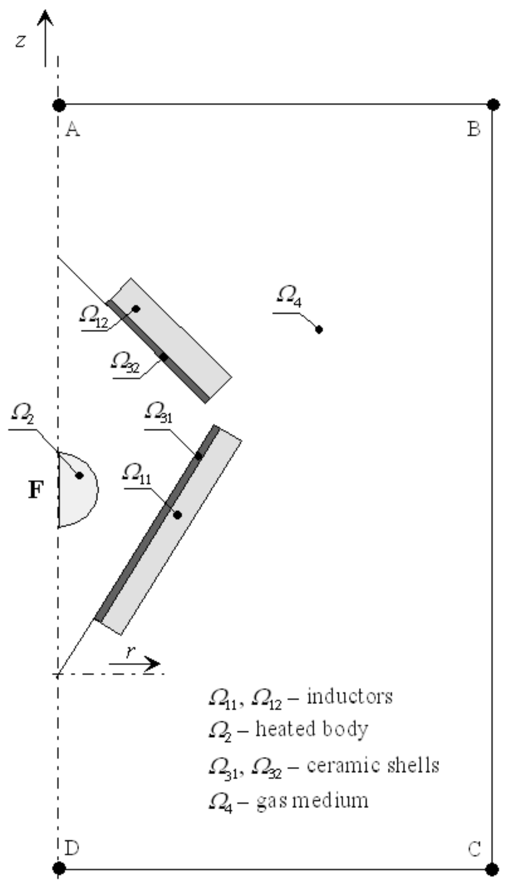

Fig. 2 Definition area of the problem

The calculated distribution of the phasor of vector potential $\underline{A}_\varphi = \underline{A}_\varphi(r,z)$ provides distribution of eddy currents $\underline{J}_{\mathrm{eddy},\varphi}$, specific Joule losses p_{J} and average specific Lorentz forces $\boldsymbol{f}_{\mathrm{L}}$ acting on the heated body. These quantities are described by relations [6]

$$\underline{J}_{\mathrm{eddy},\varphi} = -\mathrm{j}\cdot\omega\gamma\underline{A}_\varphi\,, \tag{3}$$

$$p_{\mathrm{J}} = \frac{\underline{J}_{\mathrm{eddy},\varphi}\cdot\underline{J}^*_{\mathrm{eddy},\varphi}}{\gamma} \tag{4}$$

and

$$\boldsymbol{f}_{\mathrm{L}} = \boldsymbol{J}_{\mathrm{eddy}} \times \boldsymbol{B} \tag{5}$$

where $\underline{J}^*_{\mathrm{eddy},\varphi}$ is the complex conjugate to $\underline{J}_{\mathrm{eddy},\varphi}$. Now we will try to analyze the last expression for $\boldsymbol{f}_{\mathrm{L}}$. It can be shown that

$$\boldsymbol{f}_{\mathrm{L}} = \underline{\boldsymbol{J}}_{\mathrm{eddy}} \times \underline{\boldsymbol{B}}^* = \underline{\boldsymbol{J}}_{\mathrm{eddy}} \times \mathrm{rot}\, \underline{\boldsymbol{A}}^* = \\ = \mathbf{r}_0 \cdot \frac{\underline{J}_{\mathrm{eddy},\varphi}}{r} \cdot \frac{\partial}{\partial r}\left(r \underline{A}^*_\varphi\right) - \mathbf{z}_0 \cdot \underline{J}_{\mathrm{eddy},\varphi} \cdot \frac{\partial \underline{A}^*_\varphi}{\partial z}. \tag{6}$$

The total Lorentz force $\boldsymbol{F}_{\mathrm{L}}$ acting on the body has only one nonzero component $F_{\mathrm{L}z}$ in the axial direction given by integral

$$F_{\mathrm{L}z} = \int_{V_3} f_{\mathrm{L}z} \cdot \mathrm{d}V = -\int_{V_3} \underline{J}_{\mathrm{eddy},\varphi} \cdot \frac{\partial \underline{A}^*_\varphi}{\partial z} \cdot \mathrm{d}V \tag{7}$$

where V_3 is the volume of the heated body.

The *nonstationary temperature field* is calculated only inside the heated body, i.e. in domain Ω_2 (even when its calculation within both field coils would represent no complication). The Fourier-Kirchhoff equation describing its distribution reads [7]

$$\mathrm{div}\left(\lambda \cdot \mathrm{grad}\, T\right) = \rho c \cdot \frac{\partial T}{\partial t} - p_{\mathrm{J}} \tag{8}$$

where λ denotes the thermal conductivity, ρ the specific mass of the heated material and c its specific heat. In the cylindrical coordinates we have

$$\frac{1}{r}\left(\frac{\partial}{\partial r} \lambda r \frac{\partial T}{\partial r}\right) + \frac{\partial}{\partial z}\left(\lambda \frac{\partial T}{\partial z}\right) = \rho c \frac{\partial T}{\partial t} - w_{\mathrm{J}} \,. \tag{9}$$

The corresponding boundary conditions are (see Fig. 2):

- axis of symmetry the Neumann condition $\dfrac{\partial T}{\partial r} = 0,$
- elsewhere convection and radiation expressed as $-\lambda \cdot \dfrac{\partial T}{\partial z} = \alpha\left(T - T_{\mathrm{ext}}\right) + \sigma C\left(T^4 - T_i^4\right)$

where α is the convective heat transfer coefficient, T_{ext} the known temperature of ambient medium, σ the Stefan-Boltzmann constant, C coefficient of emissivity and T_i the average temperature of the surface of the inductor.

4. ILLUSTRATIVE EXAMPLES

4.1. Input data

For the particular arrangement depicted in Figs. 1 and 2, whose most important dimensions are shown in Fig. 3, it is necessary to find the final position **S** of the heated body (and some parameters of the process of heating, particularly its velocity).

The basic data (see Fig. 3) are:

- $r_1 = 0.055$ m, $l = 0.178$ m, $N_1 = 36$, $N_2 = 18$ $s_1 = 0.011$ m, $s_2 = 0.01$ m, $\beta = 30\,°$, $\varphi = 0\,°$, $\delta = 0.052$ m,
- current densities: $J_1 = 4.67 \cdot 10^7$ A/m², J_2 varies, $f = 5$ kHz.

The coils are made from a hollow copper (Cu 99) conductor (internal diameter 4 mm, external diameter 8 mm), intensively cooled by water. Their electrical conductivity $\gamma_{\mathrm{Cu}} = 5.7 \cdot 10^7$ S/m, $\mu_{\mathrm{r}} = 1$.

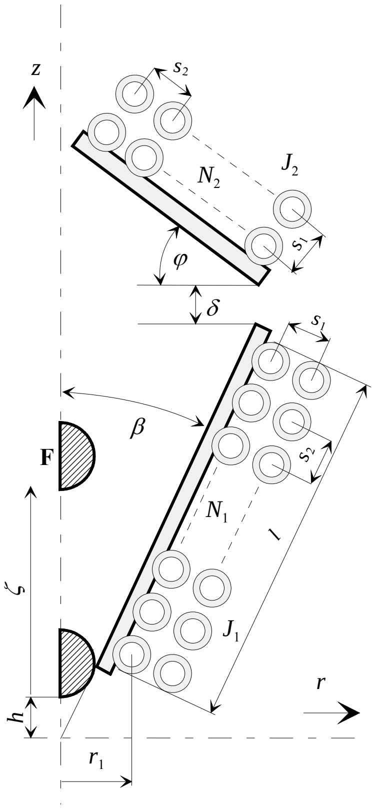

Fig. 3 Details of the system

The heated bodies are aluminum workpieces (Al 99.5, $\gamma_{\mathrm{Al}} = 3.4 \cdot 10^7$ S/m, $\lambda = 229$ W/mK, $\rho = 2700$ kg/m³, $c = 896$ J/kgK, $\mu_{\mathrm{r}} = 1$) of mass $m = 1$ kg and volume $V = 0.00037037$ m³.

- Sphere: radius $R = 0.04455$ m.
- Cylinder: radius $R = 0.03892$ m, height (that is supposed to be equal to $2R$) $H = 0.07884$ m.
- Truncated cone: smaller radius $R_1 = 0.03$ m, larger radius $R_2 = 0.0474$ m, height (that is supposed to be equal to its mean diameter, thus $R_1 + R_2$) $H = 0.0774$ m.

Temperature $T_{\mathrm{ext}} = 20$ °C, $T_{\max} = 650$ °C, coefficient $\alpha = 20$ W/m²K .

4.2. Computations

Computations were performed by professional program QuickField 5.0 supplemented by a number of single-purpose user procedures developed and written by the authors. Their order was as follows:

- Computation of magnetic fields in two selected arrangements in order to determine the position of the artificial boundary ABCD (see Fig. 2).
- Consequent computation of the same arrangements on various meshes in order to find such a density of the mesh that would ensure sufficient geometrical convergence of the results.
- Computations of the static characteristics of particular arrangements and determination of the stable positions of the body.
- Computation of the time evolution of the average temperature of the body.

4.3. Results

The first two points provided information that the artificial boundary should be placed at a distance of about 0.3 m from the coils and the discretization mesh should contain about 130000 elements.

Then we calculated the static characteristics (dependence of the total Lorentz force acting on the body on coordinate ζ, Fig. 3) of the system for the case when only the lower field coil carries current of density $J_1 = 4.67 \cdot 10^7$ A/m^2. The results are presented in Fig. 4. Fig. 5 shows the total Joule losses P_J (volume integral of (4)) in the body also as a function of position ζ

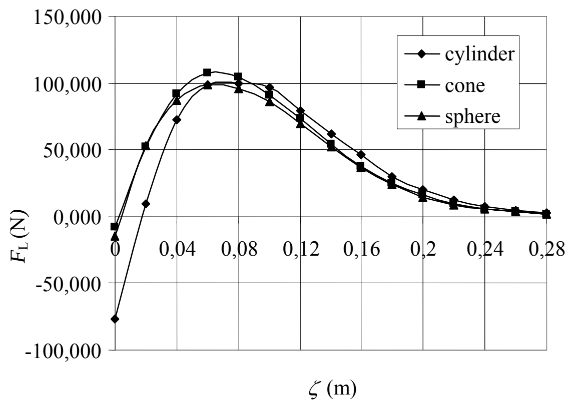

Fig. 4: Static characteristics of the system for different bodies for $J_1 = 4.67 \cdot 10^7$ A/m^2, $J_2 = 0$

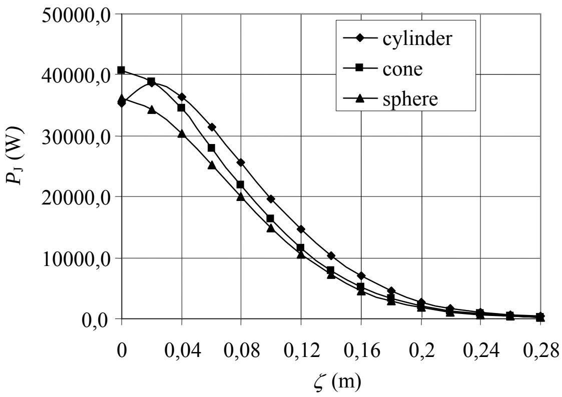

Fig. 5: Total Joule losses in the body as a function of position ζ for $J_1 = 4.67 \cdot 10^7$ A/m^2, $J_2 = 0$

Fig. 6 depicts the time evolution of the average temperature of all bodies

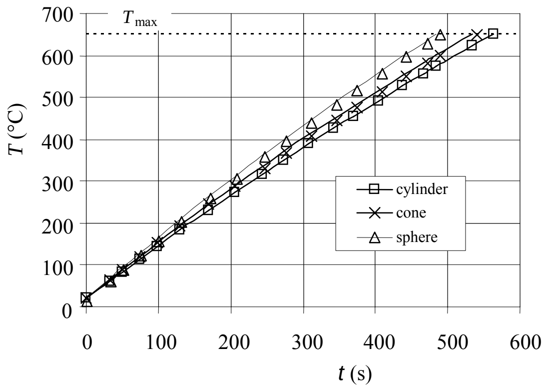

Fig. 6: Time evolution of the average temperature of all bodies ($J_1 = 4.67 \cdot 10^7$ A/m^2, $J_2 = 0$)

Table I contains the balance positions for particular bodies, corresponding Joule losses and the time t_{650} necessary for their heating to the average temperature $T_{max} = 650$ °C.

Body	Balance position ζ_0 (m)	Total Joule losses (W)	Time t_{650} (s)
cylinder	0.2303	1353	564
cone	0.2197	1251	534
sphere	0.2172	1167	484

Tab. I Balance positions, Joule losses and times t_{650} for the bodies ($J_1 = 4.67 \cdot 10^7$ A/m^2, $J_2 = 0$)

It is obvious that this way of heating is not effective. The balance positions of particular bodies do not correspond from far to positions characterized by the highest Joule losses, which is caused by their higher distance from the low coil. That is why it is necessary to use two inductors.

For the second example we selected nonzero currents in both inductors and the results are depicted in the following figures.

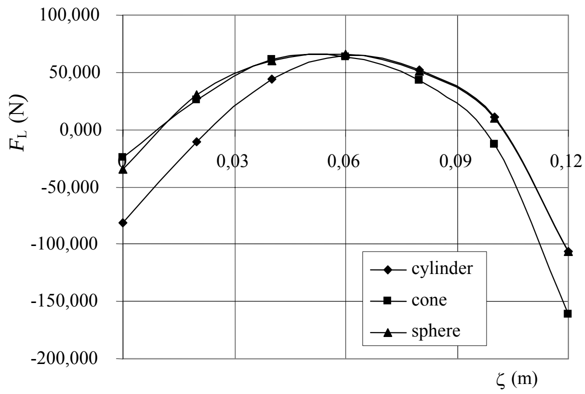

Fig. 7: Static characteristics for different bodies for $J_1 = 4.67 \cdot 10^7$ A/m^2, $J_2 = 6.67 \cdot 10^7$ A/m^2, phase shift 0 °

While current density J_1 remains the same as in the previous case, current density J_2 is now $6.67 \cdot 10^7$ A/m^2 and its phase shift with respect to J_1 is zero. Fig. 7 depicts the static characteristics of the system, Fig. 8 the total Joule losses in the bodies as functions of the position and Fig. 9 the evolution of the average temperatures of all bodies.

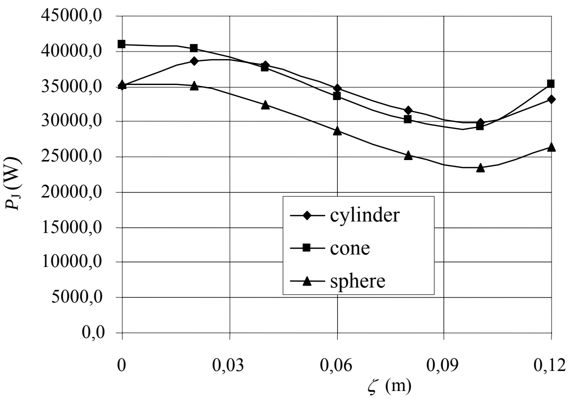

Fig. 8: Total Joule losses in the body as a function of ζ for $J_1 = 4.67 \cdot 10^7$ A/m^2, $J_2 = 6.67 \cdot 10^7$ A/m^2, phase shift $0°$

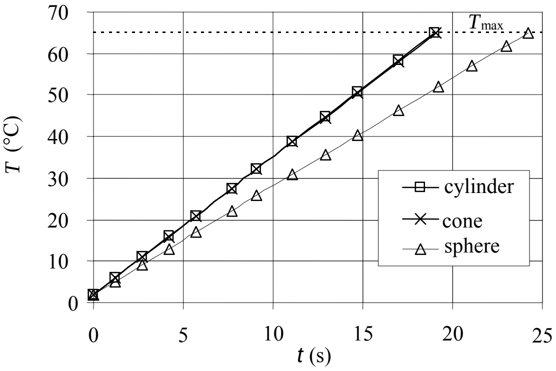

Fig. 9 Time evolution of the average temperature of all bodies, $J_1 = 4.67 \cdot 10^7$ A/m^2, $J_2 = 6.67 \cdot 10^7$ A/m^2, phase shift $0°$

Table II contains the balance positions for particular bodies, corresponding Joule losses and the time t_{650} necessary for their heating to the average temperature $T_{max} = 650$ °C.

Body	Balance position ζ_0 (m)	Total Joule losses (W)	Time t_{650} (s)
cylinder	0.1003	29808	19.0
cone	0.0919	29681	19.1
sphere	0.1000	23493	24.2

Tab. II Balance positions, Joule losses and times t_{650} for the bodies ($J_1 = 4.67 \cdot 10^7$ A/m^2, $J_2 = 6.67 \cdot 10^7$ A/m^2), phase shift $0°$

It is clear that heating of the body is approximately 25 times shorter than in the previous case. This is especially caused by the fact that the balance position is characterized by high Joule losses whose values are much more uniform than in the previous case.

The third example shows the differences when the field current in the upper coil remains the same as in the previous case, but its phase shift is $180°$ (magnetic field is now transversal while in the previous case it was longitudinal).

Fig. 10 shows the static characteristics of the system

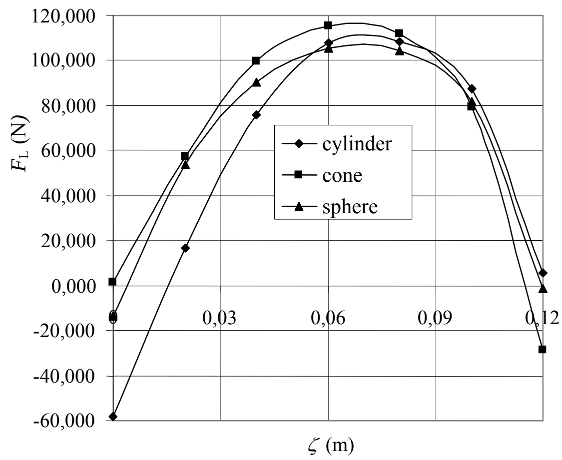

Fig. 10 Static characteristics for different bodies for $J_1 = 4.67 \cdot 10^7$ A/m^2, A/m^2 $J_2 = 6.67 \cdot 10^7$ A/m^2, phase shift $180°$

Fig. 11 shows the distribution of the total Joule losses produced in the bodies as a function of their position.

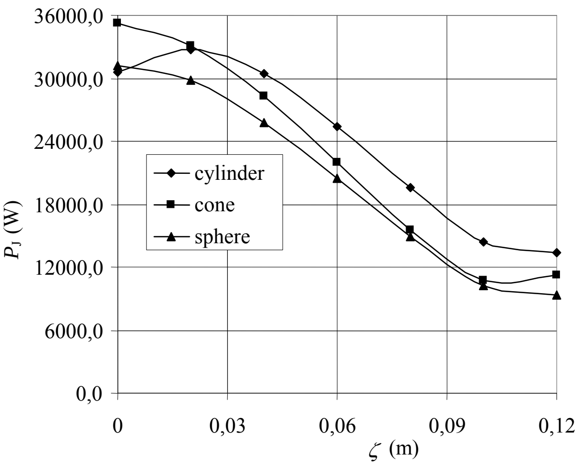

Fig. 11 Total Joule losses in the body as a function of ζ for ($J_1 = 4.67 \cdot 10^7$ A/m^2, $J_2 = 6.67 \cdot 10^7$ A/m^2), phase shift $180°$

And finally Fig. 12 shows the evolution of the average temperatures inside the bodies and table III summarizes the corresponding results.

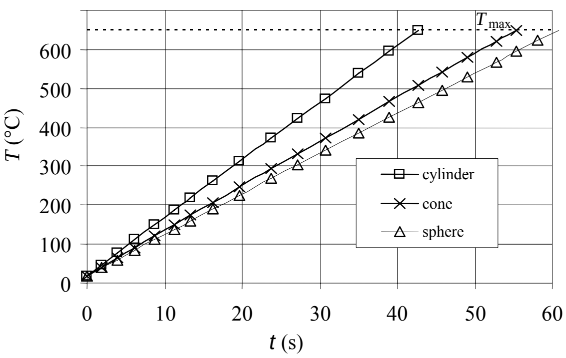

Fig. 12 Time evolution of the average temperature of all bodies, $J_1 = 4.67 \cdot 10^7$ A/m^2, $J_2 = 6.67 \cdot 10^7$ A/m^2, phase shift $180\,°$

Body	Balance position ζ_0 (m)	Total Joule losses (W)	Time t_{650} (s)
cylinder	0.1189	13391	42.7
cone	0.1129	10376	55.4
sphere	0.1173	9448	60.8

Tab. III Balance positions, Joule losses and times t_{650} for the bodies ($J_1 = 4.67 \cdot 10^7$ A/m^2, $J_2 = 6.67 \cdot 10^7$ A/m^2), phase shift $180\,°$

The decisive parameters of heating are now substantially worse, which is caused by lower Joule losses in transversal magnetic field.

5. CONCLUSION

Levitation heating is a process that depends on a lot of parameters (particularly on geometry of the device and heated body and also on currents in individual inductors and their phase shifts). The paper shows how the results depend on several of them. For the given arrangement the optimal version is heating of a cylinder in longitudinal magnetic field (there is no phase shift between both currents).

Next research in the field will be aimed at investigation of the influence of the shape of both inductors and attention will also be paid to mapping of the mechanical transient that is a function of the initial distance between the starting and final positions of the heated body and damping in inert atmosphere under pressure.

ACKNOWLEDGEMENT

Financial support of the Grant Agency of the Czech Republic (Project No. 102/04/0095) is gratefully acknowledged.

REFERENCES

[1] Doležel, I., Dvořák, P., Mach, M., Ulrych, B.: Comparison of Systems for Levitation Heating of Electrically Conductive Bodies. Advances in Electrical and Electronic Engineering, No. 2, Vol. 3, 2004, pp. 161–166.

[2] Doležel, I., Karban, P., Mach, M., Musil, L., Ulrych, B.: Dynamic Characteristic of Aluminum Sphere Levitating in Electromagnetic Field Respecting its Induction Heating. Proc. CPEE'2004, 1.–4. 9. 2004, Zakopane, Poland, pp. 1–4.

[3] Doležel, I., Mach, M., Ulrych, B.: Induction Heating of Metal Cylinder Levitating in Harmonic Electromagnetic Field. Technical Electrodynamics, Proc. PPE Kiev 2004, Vol. 3, pp. 3–7.

[4] J. Stratton: Electromagnetic Theory, Mc Graw Hill Book Co., NY, 1941.

[5] Chari, M. V. K., Salon, S. J.: Numerical Methods in Electromagnetism, Academic Press, 2000.

[6] N. Ida: Engineering Electromagnetics. Springer, 2000.

[7] Holman, J. P.: Heat Transfer, McGraw Hill Co., 2002.

[8] www.quickfield.com.

BIOGRAPHY

Ing. Martin Mach (1980) finished his MSc studies at the Faculty of Electrical Engineering, University of West Bohemia in Pilsen, in 2003 and immediately started with the PhD studies in the Department of Theory of Electrical Engineering (supervisor Prof. Doležel). His topic is computational electromagnetics, particularly selected coupled electromagnetic-thermomechanical problems. He is an author and co-author of about 10 papers (mostly in proceedings of international conferences).

Ing. Pavel Karban (1980) finished his studies at the Faculty of Electrical Engineering, University of West Bohemia in Pilsen, in 2002. In 2003 he started doctoral studies in the Department of Theory of Electrical Engineering (supervisor Prof. Doležel). His topic is computational electromagnetics, particularly integral models for solution of low-frequency magnetic fields. He is an author and co-author of about 20 papers (mostly in proceedings of international conferences) and several large programs.

Prof. Ivo Doležel (1949) obtained his Eng. degree from the Faculty of Electrical Engineering (Czech Technical University in Prague) in 1973 and after 28 years in the Institute of Electrical Engineering of the Academy of Sciences of the Czech Republic he returned back to the Czech Technical University. His interests are aimed mainly at electromagnetic fields and coupled problems in heavy current and power applications. He is an author or co-author of one monograph, about 240 papers and several large program packages.